Derivation of future intraday price series from the outputs of energy system modelling

Ryan HARPER[1(1)], Timo KERN[(1),] Serafin VON ROON[(1)]

[(1)]FfE München

Abstract:

The intraday market is becoming increasingly important for correcting generation and load imbalances, as well as offering opportunities for arbitrage, allowing traders or operators of flexible devices to profit from price differences between temporally separated markets. To assist the development of profitable future intraday trading strategies, a methodology is presented for the modelling of prices on the hourly continuous intraday market via the stochastic generation of price differences in line with observed characteristics of historical price differences between the intraday and day ahead markets. After model validation based upon historical data, future prices are modelled based upon the outputs of the energy system model ISAaR.

Keywords: intraday trading, price uncertainty, price forecasting, Markov chain

1 Motivation

As the German energy system continues to be transformed over the course of the Energiewende, the share of electricity generated by volatile renewable sources will also continue to rise. In turn, this will result in increasing importance of, and trading on, the intraday market /RWE-01 18/. The volume of electricity traded on this market has already increased by 300 % between 2012 and 2018 /FFE-75 19/. Beyond its importance for correcting generation and load imbalances, intraday trading also offers opportunities for arbitrage, allowing traders or operators of flexible devices to profit from price differences that may emerge between the day-ahead and intraday markets or between the intraday auction and continuous trading /WUT-01 19/ /FFE-69 15/. Successfully capturing these revenues is key to integrating flexible units, such as electric vehicles capable of bidirectional charging, into the energy system and smoothing the volatility of renewable generation /FFE-116 20/. To assist the development of profitable future intraday trading strategies, prices on the continuous intraday market will be derived from modelled future prices, obtained from the FfE energy system model ISAaR /FFE-118 19/, for the year 2030.

[1] Am Blütenanger 71, 80995 München, +49 (0)89 158121-67, rharper@ffe.de

2 Methods

A time series of continuous intraday electricity prices[2] is generated, first using historical data and a Markov chain for the stochastic selection of price deviations, before the method is extended to the future using the results of energy system modelling. An overview of the methods used can be seen in Figure 1. The individual steps will be briefly described here before further detail is provided in the following sections.

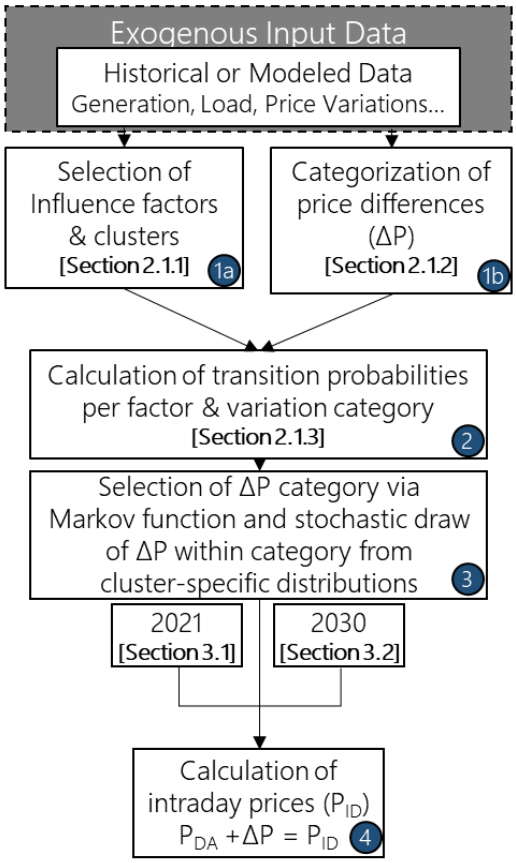

Figure 1: Overview of modelling steps

The historical input data includes conventional and renewable generation, load, residual load, and day-ahead electricity prices from EPEX and ENTSO-E /EPE-01 19/ /ENTSOE-01 20/. The influence of such factors upon the variations between day ahead and intraday prices (ΔP) are examined using additional historical time series data from 2018-2021, and relevant factors are selected for the determination of future prices (Step 1a in Figure 1 – see section 2.1.1). The historical price variations under consideration of various levels of the influencing factors (e.g., high vs. low residual load) are also categorized (e.g., high/low negative variation, high/low positive variation) in Step 1b (see section 2.1.2 & 2.1.3). The factors, their levels, and the variation categories are carried over for the modelling of stochastic price differences.

To obtain stochastic price differences within the ranges of the observed variation categories, and to reflect the temporal linkages between price variations of consecutive time steps, the

[2] In this paper, intraday prices refer to the volume-weighted average price of all transactions in continuous intraday trading within 3 hours before delivery, or the ID3 Price.

price variations will be drawn using a Markov chain. Transition probabilities for each variation category are calculated from the historical data for all levels of each selected influence factor (Step 2 in Figure 1: Overview of modelling steps – see section 2.1.3). For each time step the current state of the influencing factor, historically observed or as modeled in ISAaR, and the category of the price variation from the previous time step together determine which transition probability from step 2 is used by the Markov function. After the category of price difference is determined via the Markov function, a new price difference is drawn from a cluster-specific distribution reflecting the historical observed differences in step 3. These price differences are then summed with the corresponding day-ahead prices from the historical dataset or from ISAaR in step 4 to obtain a time series of continuous intraday prices. This paper describes the calculation of hourly continuous intraday prices based on deviations from the day-ahead market, but the method can be used in the same manner to obtain quarter-hourly continuous prices using deviations.

The following sub-chapters will describe the individual steps of the methodology in more detail.

2.1.1 Situation-dependent intraday price uncertainty

For the selection of influence factors, historical time series data from the years 2018-2021 was examined in an extension of analyses conducted in /FFE-75 19/. In this previous work, potential influence factors were chosen which display both a systematical influence on prices and can be evaluated based on data available during day-ahead trading to account for uncertainty at gate closure. In addition to the weekday and time of day, day-ahead forecasts of load, generation from wind and PV, and residual load (load not met by volatile generation from wind or PV) were selected as influencing factors. Similarly to /FFE-75 19/, the standard deviation of the price difference between day-ahead and intraday prices in a variety of different market situations was analyzed, in this case with data from 2019-2021 in addition to the 2018 data used in the previous analysis. The standard deviation (s) of the price difference between the day-ahead price and the id3 price of hourly continuous trading in different extremities of each influence factor can be seen in Figure 2.

Day of the week and load can quickly be dismissed as potential influence factors, as the different levels seem to display no clear pattern that would explain differing standard deviations. For instance, although Tuesdays demonstrate a markedly higher mean standard deviation, there is no clear reason as to why this should be the case.

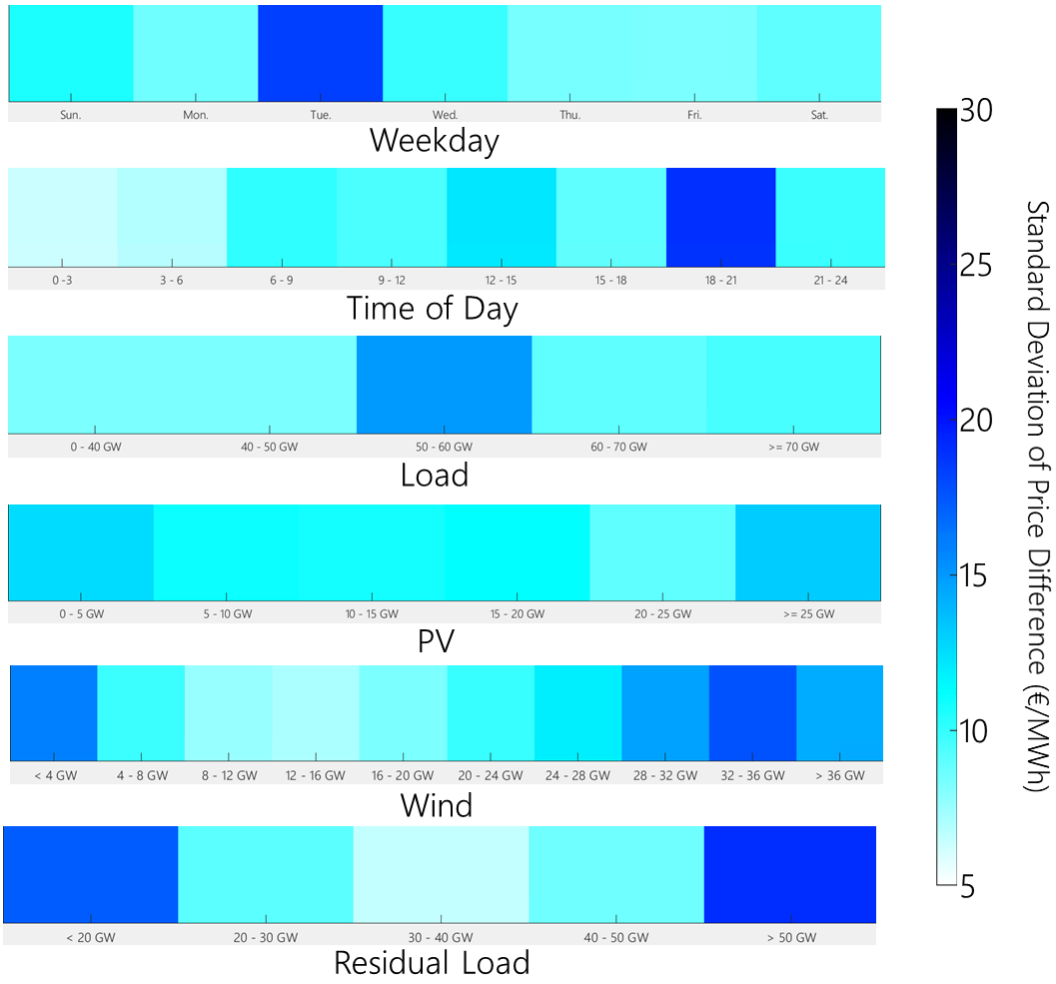

Figure 2: Situation-dependent intraday price uncertainty. Standard deviation of price differences between the intraday and day ahead prices, clustered by situational characteristics

Similarly, no clear reason can be deduced that explains both the more volatile price deviations in the load category 50-60 GW (**s** = 15 €/MWh) and would also account for more stable price deviations across all other load categories (**s** = 8.3 to 9.6 €/MWh).

Clearer patterns emerge in many of the other categories. Among the time-of-day clusters, a higher standard deviation of price differences aligns with the evening load peak, while more stable prices (lower standard deviations) are seen during the overnight hours. Wind and PV generation both display higher deviations at low and high levels of forecast generation, while more moderate forecasts are associated with a lower standard deviation of price differences. Particularly for forecast wind generation, a rising standard deviation accompanies increasing generation forecasts for many of the forecast ranges as visible in Figure 2. Increasing likelihood of curtailment at higher levels of wind generation, until curtailment is almost assured at the highest levels of forecast generation and therefore less uncertain, offers one potential explanation for this phenomenon.

The final influencing category, residual load, similarly displays significantly higher standard deviation of price differences at low (< 20 GW; **s** = 17.2 €/MWh) and high (> 50 GW; **s** = 15.1 €/MWh) levels of residual load than in the three middle clusters (**s** = 9, 6, and 8.6 €/MWh). Such a systemic pattern may be explained by the characteristics of

the present merit order. At moderate levels of residual load, the price-setting units are likely of similar nature, including relatively comparable costs, meaning a movement along the supply curve results in a smaller effect on the market price. Meanwhile, at both ends of the supply curve, there are rapid jumps in costs of supply as one moves from price setting via renewables to conventional generation at lower levels of demand and to more expensive fuel sources or peaking units at high levels of demand.

As an influencing category, residual load offers the advantage of combining the effects of multiple other categories. Rather than attempting to assess the influence of load, wind generation, and PV generation separately, the residual load captures the interactions between these categories. For further analyses within this paper, residual load will be used as the influencing factor and will be divided into three clusters: Low (< 20 GW), Mid (20-50 GW), and High (> 50 GW).

2.1.2 Temporal interdependencies of intraday price uncertainty

For the modeling of a Markov process, a matrix of transition probabilities must be constructed. These describe the probability of moving from a given state in one timestep to a different state in the following time step. To construct such a matrix, the individual states must be defined and the probability of moving from each one to all others must be calculated. In this case, different states of ΔP, the price difference between the day ahead and intraday market prices, will be considered in a first-order Markov chain, or a stochastic process in which the new state is influenced only by the state immediately preceding it. /ALUF-02 16/

Examining historical data from the years 2018-2021[3], as depicted in Figure 3, reveals that for a large proportion of hours the price difference between the day ahead and intraday prices (ΔP) was between -10 €/MWh and 10 €/MWh.

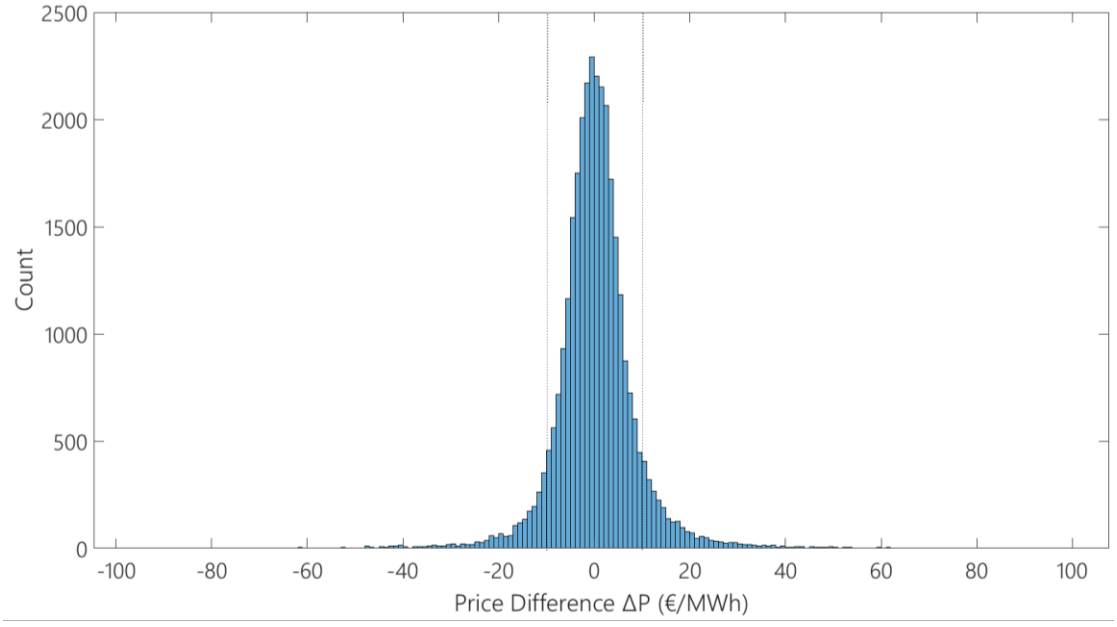

Figure 3: Distribution of observed hourly price differences ID3-DA 2018-2021. Dotted vertical lines indicate -10 €/MWh and 10 €/MWh

[3] For 2021, data from January 1st to August 31st

Further examinations quantified this large proportion, with the price difference in 86 % of hours falling into this 20 € band. With the goal of minimizing the number of transition probabilities that must be applied when using the Markov chain, the price variation categories were limited to the four depicted in Figure 4; High and low positive and negative variation, where high variation refers to a price difference with an absolute value larger than 10 €/MWh, and low variation refers to a price difference with an absolute value between 0 and 10 €/MWh.

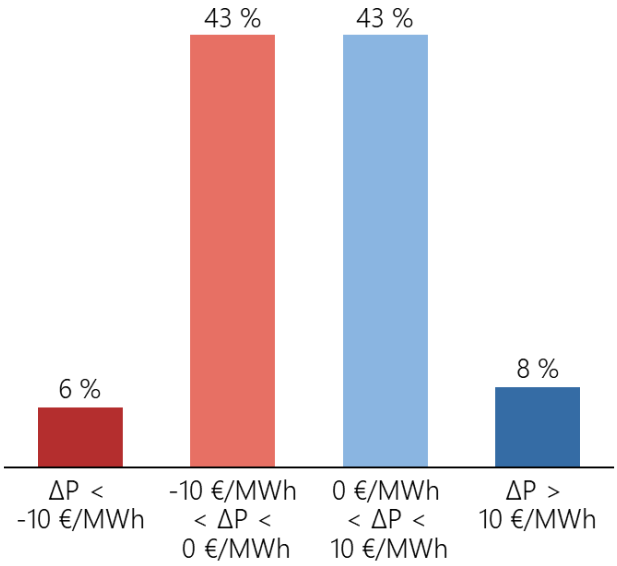

Figure 4: Shares of hours within each price variation category

In the following step, the historical data was examined for evidence of correlation between the price difference of a given hour and that of the previous hour. Figure 5 depicts the results of this examination. For each variation category of ΔP (Z1…4) in an initial hour (H_t), as represented in the top row of large circles, the frequency of each variation category in the following hour (H_{t+1}) was calculated. These shares are depicted in the second row in circles of the respective color, with the largest circle representing the category with the largest share of following hours. As a concrete example, in hours in which ΔP fell within category Z1, ΔP remained in this category in the next hour in 63 % of all cases and transitioned to category Z2 in 34 % of cases.

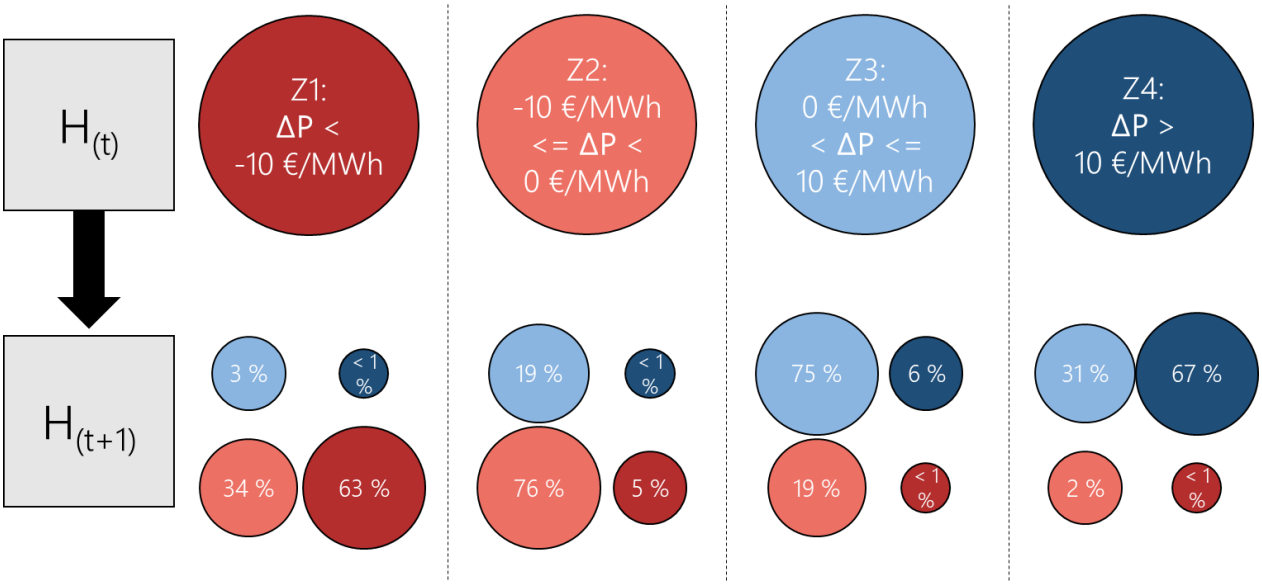

Figure 5: Transition probabilities from a given state in H_t to each of the four states in the following hour H_{t+1}

Two trends are apparent upon examining these results: Remaining within the same category is the most common outcome for H_{t+1} over all categories, and changes of category occur largely in the direction of ΔP = 0, whether from a high to low absolute variation (e.g., Z4 → Z3) or from a low positive to a low negative variation (e.g., Z3 → Z2). More importantly, these results strongly suggest that there is a correlation between the state of ΔP between a timestep and the following timestep, indicating that the first order Markov chain provides an appropriate tool for the generation of stochastic price differences.

These transition probabilities represent the dataset as a whole, however the analysis of the influencing factor residual load described in section 2.1.1 demonstrated that periods with low or high residual load are associated with higher standard deviations of ΔP, or more volatile prices. This suggests that the transition probabilities should be calculated separately depending on the residual load of the current timestep H_t.

The calculated transition probabilities for the three residual load clusters can be seen in Figure 6. A comparative table, including all differences of the cluster-specific transition probabilities to the pooled transition probabilities, can be found in the appendix as Table 4.

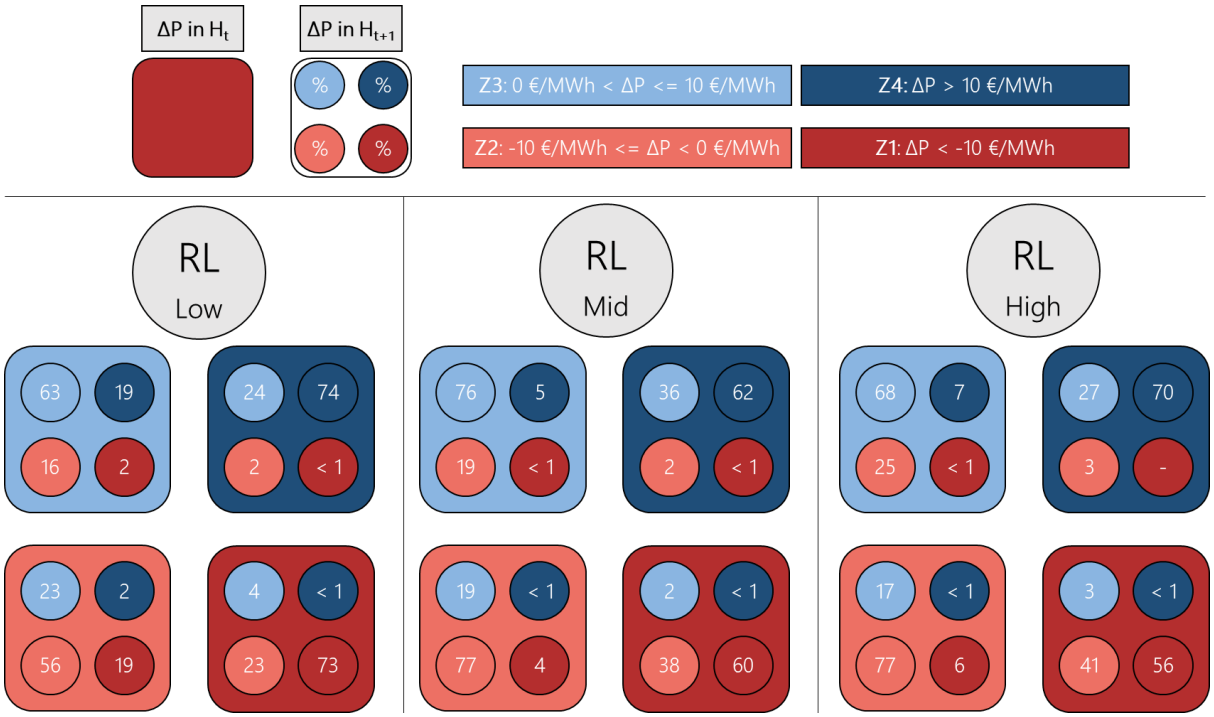

Figure 6: Cluster-specific transition probabilities for the four states of ΔP (Z1-4) in each of the defined residual load clusters.

These calculations confirm that the use of cluster-specific transition probabilities is necessary. The difference between the pooled and cluster-specific transition probabilities is particularly notable for cluster low, in which the probability of obtaining ΔP from Z1 or Z4 (absolute value of ΔP > 10 €/MWh) in H_{t+1} increased for all starting categories. The largest increases were Z2 → Z1 (+13 percentage points) and Z3 → Z4 (+14 percentage points). Meanwhile, cluster high shows an increased tendency to revert from large absolute price differences to smaller ones, and to transition from a small positive to a small negative price difference. The transition probabilities of cluster mid closely resemble the overall sample. The use of these cluster-specific transition probabilities will enable the generation of price differences more in line with the observed characteristics of the market.

2.1.3 Modeling time series and situation dependent price uncertainty of continuous intraday trading

After the state of ΔP in H_{t+1} is stochastically determined by the Markov chain based upon the calculated transition probabilities described above, the new ΔP will also be selected via a random draw. These new price differences should reflect the distribution of price differences observed within the four states among the historical data.

Recalling the distribution of the historical price differences seen in Figure 3Figure 4, a simple visual analysis already begins to suggest that the data is not normally distributed. Overlaying the data with a normal distribution function, fitted by maximum likelihood estimation, allows for further graphical analysis and confirms this initial suggestion. As can be seen in Figure 7, a normal distribution function (dashed line) does not fit large areas of the historical data well. This graphical analysis is also confirmed by the Kolmogorow-Smirnow test /ÖZT-01 06/, which rejects the hypothesis that the data represents a normal distribution.

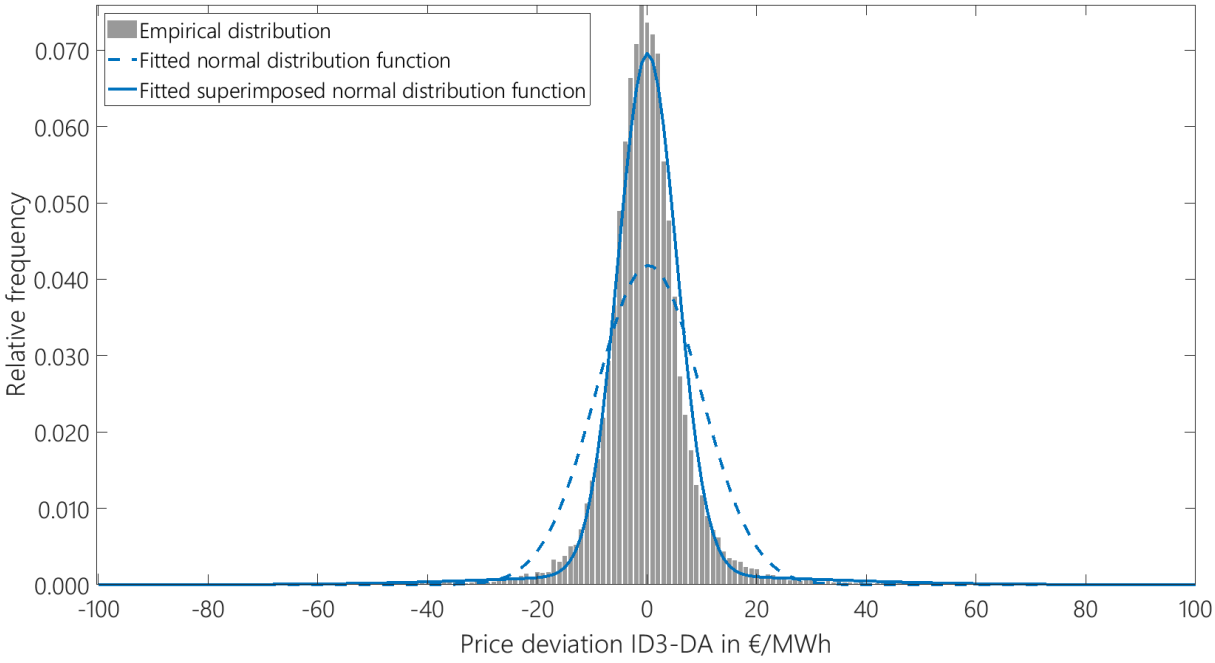

Figure 7: Relative frequency of price differences among the observed empirical distribution and comparison to fitted distribution functions

To better fit the data, a superimposed normal function (solid line in Figure 7) was created via the additive mapping of two normal functions and fit again by maximum likelihood estimation. The first function has a very small standard deviation to better represent the high numbers of observations at low price differences. The second function has a higher standard deviation to represent long tails of the distribution which contain higher price differences. Although the superimposed function fits the data better visually, some areas are still poorly represented and the Kolmogorow-Smirnow test still rejects the hypothesis that the observed data could have come from the superimposed distribution function. The peak and shoulders of the superimposed function offer the most noticeable differences to the historical distribution.

As the Kolmogorow-Smirnow test tends to be very sensitive when applied to large sample sizes /NAA-01 11/, further investigation of the quality of the superimposed function was performed using the probability density curves of both functions. As can be seen in Figure 8, the cumulative distribution of the superimposed function is a much closer match to that of the observed data than the normal function. Therefore, the imperfections of the superimposed function were accepted, and the function is used to generate the stochastic deviations during the simulation. Using an individually-defined function to reflect the distribution within each of the three residual load clusters, a large pool of price differences is created for each of the three residual load clusters. For each timestep, a new price difference is then selected at random from the appropriate pool based upon the state of ΔP determined by the Markov function.

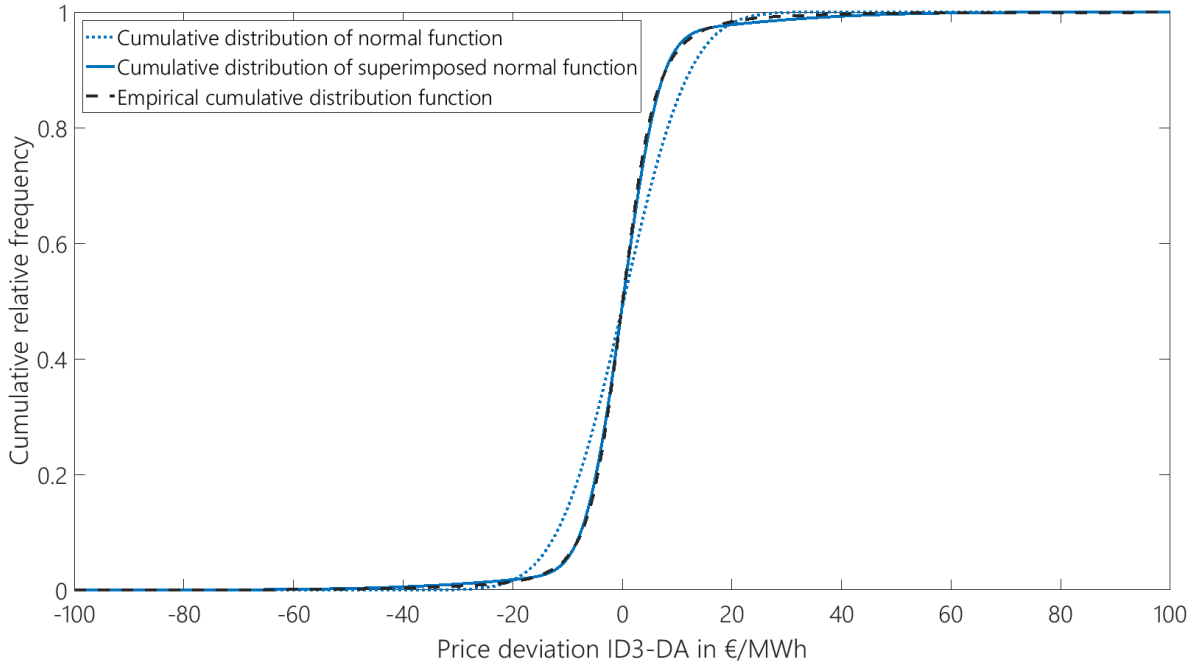

Figure 8: Comparison of cumulative relative frequency of price differences among the empirical, normal, and superimposed normal distribution function

3 Results

With the transition probabilities and appropriate distributions for the drawing of new price differences per residual load cluster in place, the method was first tested using the historical dataset before being applied to the 2030 modelling results.

3.1 Model validation: Modeling characteristics of historical intraday price uncertainty

The data from 2018, 2019, and 2020 was used as a training dataset to calculate transition probabilities[4], which were then used along with the historical day-ahead prices and residual load from 2021 to generate stochastic price differences. Three days of simulated price differences is compared with the observed historical deviations in Figure 9.

As to be expected with a stochastic drawing of ΔP, the simulated values do not match the historical values. However, with the assistance of the colored bands indicating the hourly residual load forecast, visual analysis suggests that the characteristics of the price differences seen in the historical data are well reproduced in the simulated values.

Overall, ΔP falls largely within the anticipated band from -10 €/MWh to 10 €/MWh. Those hours with larger price differences correspond to the hours of low residual load, in which larger price differences were shown to be more common. Within the low-variation categories Z2 and Z3, ΔP also generally retains the same sign, only occasionally springing from positive to negative or vice versa. When compared with price differences drawn at random from a distribution with

[4] Not presented separately. Maximum difference from transition probabilities of the 2018-2021 pooled dataset is +/- 4 percentage points.

a standard deviation and mean equal to those of the observed 2021 price differences, the influence of the residual load clusters and time effects when drawing ΔP become apparent. The random price differences demonstrate a stronger sawtooth pattern than the modeled price differences, as well as more frequent price differences of categories Z1 and Z4 while in the residual load cluster middle.

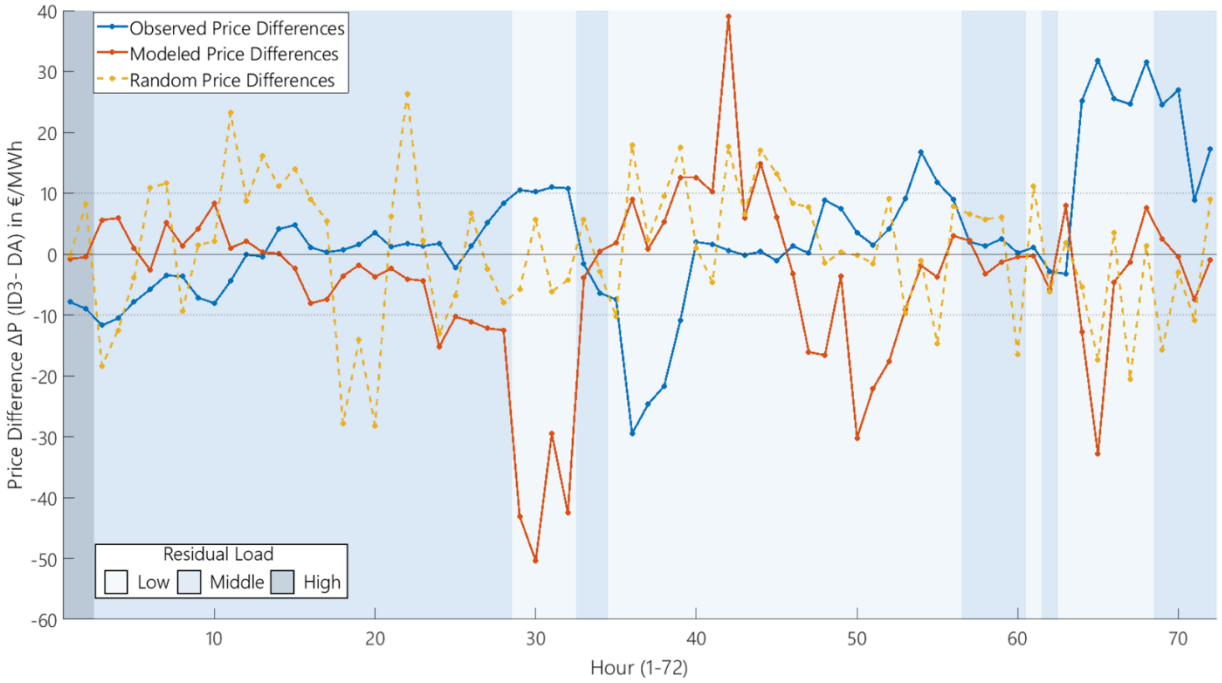

Figure 9: Exemplary 72 hours comparing modeled, observed, and randomly drawn ΔP for the year 2021

To complement the visual analysis of a single day, the standard deviations of all hours from the three depicted time series are presented in Table 1.

Table 1: Standard deviation of observed price differences for 2018 - 2020 without clusters (used for the drawing of random price differences), observed price differences by cluster for 2021, and 100 modeled time series for the year 2021 based upon observed price differences with clusters from 2018 - 2020.

	Random Draws (2018-2020 without Clusters)	Observed Values (2018 - 2020)			Mean of 1000 Model Results		
Standard Deviation of ΔP (€/MWh)	-	Low	Mid	High	Low	Mid	High
	11.1	17.1	7.6	19.9	16.3	8.2	17.7

The characteristics of the training dataset are reasonably well reproduced in the model results. As discussed in section 2.1.3, the modeled distribution matches the historical distribution less well in the peak and shoulders of the distribution. This is particularly noticeable in the lower standard deviation of cluster mid within the observed historical data, due to the influence of a larger share of small absolute price differences compared to the modeled values. In addition, the standard deviations of clusters low and high within the observed historical data were impacted by a small number of very large absolute price differences. The very low probability of drawing such price differences from the modeled distributions in turn leads to lower standard

deviations for these clusters in the model results. Despite these weaknesses, a clear benefit of the model versus the drawing of random price differences is observable when comparing the cluster-specific standard deviations with the pooled standard deviation of ΔP.

The volatility of the price differences was also examined as a means of evaluating the model results. Here the share of hours in which ΔP exhibits a different sign than the previous hour and the mean number of hours between sign switches were examined. The results are displayed in Table 2.

Table 2: Comparison of price difference volatility

	% Of Hours With a Sign Switch	Mean Duration Between Sign Switches
Random Draws	49.9 %	2 Hours
Observed Values 2018-2020	16.6 %	6.02 Hours
Mean of 1000 Model Results	16.5 %	6.04 Hours

These results suggest a good reproduction of the observed temporal effects between timesteps within the model. As was evident from the sawtooth pattern seen in the previous visual analysis, a random draw leads to much more frequent changes from positive to negative price differences (or vice-versa) compared to the observed values. The model results reflect the observed values much more closely.

3.2 Modeling future intraday price uncertainty

Taking the reproduction of the temporal and cluster-specific characteristics of the training dataset in the modeled year 2021 as a successful proof of concept, this method was then applied to the results of the ISAaR Energy system model for the year 2030 based on climate target scenario solidEU of FfE project eXtremOS /FFE-23 21/. The linear optimization model ISAaR supplies a time series of day-ahead prices based on marginal cost of generation units in the energy system and residual loads /FFE-118 19/, which are used along with the calculated transition probabilities (2018-2021) presented in section 2.1.2 to draw price differences for the continuous intraday market.

The results for 2030 are markedly different than those for 2021. After 1000 model iterations for each year, the mean standard deviation of ΔP increased by 5 €/MWh in 2030 compared to 2021. The distribution of the standard deviation of ΔP in each of the model iterations is depicted in Figure 10.

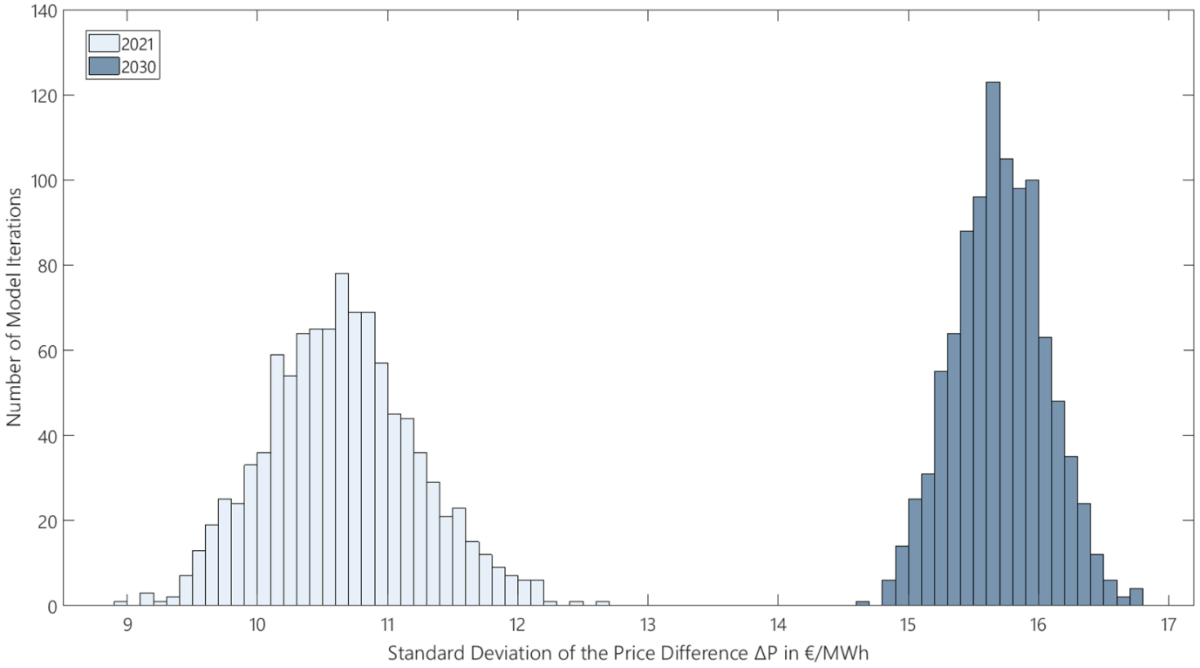

Figure 10: Histogram depicting the distribution of the standard deviation of ΔP across 1000 model iterations for 2021 and 2030

The key explanation for the new characteristics can be found in the residual load clusters. As can be seen in Table 3, while the residual load cluster middle is the most common status among the 2021 hours (79 % of hours), this is replaced by residual load cluster low in the 2030 dataset (69 % of hours). This is the result of a strong expansion of renewable generation capacity within the ISAaR energy system model, leading to more frequent hours with low or negative residual load. In turn, the cluster-specific transition probabilities within the model described here lead to more hours within the states Z1 and Z4, and therefore more frequent larger absolute price differences.

Table 3: Mean Standard Deviation of P Across 1000 Model Iterations and Share of Timesteps per Residual Load Cluster for 2021 and 2030

Year	Mean Standard Deviation of ΔP across 1000 Model Iterations	Share of Timesteps per Residual Load Cluster		
		Low	Mid	High
2021	10.7	10 %	79 %	11 %
2030	15.7	69 %	24 %	7 %

4 Discussion & Conclusion

Initial analyses showed situational and temporal effects on the price differences between the Intraday and Day Ahead markets. Through the use of a Markov chain with situation-specific transition probabilities for the defined residual load clusters, both of these effects could be included in the model. The developed model generates time-series of price differences that adequately reproduce the characteristics observed in the historical dataset of observed price differences.

Further development to improve the model's reproduction of the peak and shoulders of the historical distribution can benefit the ability to reproduce the observed characteristics. In addition to considering the state of ΔP in the previous hour (Z1…4), also accounting for the magnitude of ΔP within the given state could smooth movements within a single state. While the addition of forecast errors as a further influencing factor is worth considering, this is not currently available in the data used for the modelling of 2030 here.

Two questions must be considered for the use of the presented method for the modelling of future price differences. First, is the observed temporal interdependence between the price differences of consecutive hours likely to retain its influence on the future? In the opinion of the authors, the temporal interdependences observed here are likely to remain relevant. A key reason for this belief is the assumption that forecasting errors will become more relevant for price formation as the share of renewable generation increases further. If these errors maintain the same sign (positive or negative forecasting error) over multiple hours, price differences in these hours will likely also move in the same direction. This could lead to a stronger temporal linkage than seen today.

Secondly, can the residual load clusters used here be applied as-is for the modelling of future prices? At present, times of low residual load are the result of high levels of renewable generation and are frequently characterized by the curtailment of renewables. This can cause forecast errors resulting in price instability. The increased frequency of low or even negative residual load observed in the 2030 data is in line with increasing renewable capacity in the energy system and will likely lead to a continuation or strengthening of the characteristics observed in cluster low. On the other hand, increasing experience in a renewables-dominated energy system is likely to lead to improved forecasting accuracy. With two factors working in opposite directions, the characteristic of cluster low is left unchanged at present.

In cluster mid, increasing fuel and CO2 prices are expected to transform the middle of the merit order curve from relatively flat to a much steeper curve. In turn, a forecasting error that causes a relatively small change in price as one moves along the merit order will have a larger impact upon price in the future. Cluster mid is likely to require refinement for future work. A similar effect is likely to be seen in cluster high. As the price volatility is already relatively high here, due to small numbers of large absolute price differences, the characteristic as a whole can remain unchanged.

The method presented here offers the ability to generate plausible future price differences based upon observed historical market trends. A particular advantage is the relatively low requirement for both input data and computer resources. While the results are stochastic in

nature, they are based upon statistical trends and can be used to generate corridors of potential prices via repeated simulation. A potential opportunity for expansion of the method would be exploring the effects of defining residual load clusters in relation to the maximum residual load rather than fixed levels of residual load. Additionally, the decision made here to limit the number of influence factors (one), its clusters (low/middle/high), and the number of transition states (four) in favor of computational simplicity could be reversed. Expanding any of the listed model components may allow for more precision. The extent to which this would influence the results will be explored in future work.

Literatur

ALUF-02 16 Depperschmidt, Andrej: Markovketten - Vorlesungsskript. Freiburg: Universität Freiburg, 2016.

ENTSOE-01 20 Electricity Production Data from Transparency Platform. In: https://transparency.entsoe.eu/generation/r2/actualGenerationPerProductionType/show. (Abruf am 2020-02-18); Brüssel: ENTSO-E, 2020.

EPE-01 19 Power Market Data. In: https://www.epexspot.com/en/market-data/. (Abruf am 2019); Paris: EPEX SPOT, 2019.

FFE-69 15 von Roon, Serafin et al.: Limitierte Gebote im Day-Ahead Handel als Maß für Liquidität und Preisaufschlag im Intraday-Markt. München: Forschungsgesellschaft für Energiewirtschaft mbH, 2015.

FFE-118 19 Hourly CO2 Emission Factors and Marginal Costs of Energy Carriers in Future Multi-Energy Systems (Germany): http://opendata.ffe.de/dataset/dynamis-emission-factors/; München: Forschungsstelle für Energiewirtschaft e. V. (FfE), 2019.

FFE-75 19 Kern, Timo et al.: The value of intraday electricity trading – Evaluating situation-dependent opportunity costs of flexible assets. München: Forschungsgesellschaft für Energiewirtschaft mbH, 2019.

FFE-116 20 Kern, Timo et al.: Integrating Bidirectionally Chargeable Electric Vehicles into the Electricity Markets. Basel, Switzerland: Energies 2020, 13(21), 5812, 2020.

FFE-23 21 eXtremOS Website. In: https://extremos.ffe.de. (Abruf am 2021-05-07); München: Forschungsstelle für Energiewirtschaft e. V. (FfE), 2021.

NAA-01 11 Nor Aishah Ahad et al.: Sensitivity of Normality Tests to Non-normal Data. In: Sains Malaysiana 40(6):637-641. Bangi: Universiti Kebangsaan Malaysia, 2011.

ÖZT-01 06 Öztuna, Derya et al.: Investigation of four different normality tests in terms of type 1 error rate and power under different distributions. In: Turkish Journal of Medical Sciences 36 (3): 171-176. Ankara: Ankara University, 2006.

RWE-01 18 Kath, Christopher et al.: The value of forecasts: Quantifying the economic gains of accurate quarter-hourly electricity price forecasts. Essen: RWE Supply & Trading GmbH, 2018.

WUT-01 19 Maciejowska, Katarzyna et al.: Day-Ahead vs. Intraday - Forecasting the Price Spread to Maximize Economic Benefits. Wroclaw: Wrocław University of Science and Technology, 2019.

Table 4: Transition probabilities from 2018-2021, presented as percentages for the dataset overall and for each residual load cluster. Numbers in parentheses represent the change in percentage points from the probabilities of the combined dataset.

Overall		ΔP in H_{t+1}			
		Z1	**Z2**	**Z3**	**Z4**
ΔP in H_t	**Z1**	63	34	3	<1
	Z2	5	76	19	<1
	Z3	<1	19	75	6
	Z4	<1	2	31	67
Residual Load - Low		ΔP in H_{t+1}			
		Z1	**Z2**	**Z3**	**Z4**
ΔP in H_t	**Z1**	73 (+10)	23 (-11)	4 (+1)	<1
	Z2	19 (+14)	56 (-20)	23 (+4)	1 (+1)
	Z3	2 (+2)	16 (-3)	63 (-12)	19 (+13)
	Z4	<1	2	24 (-7)	74 (+7)
Residual Load - Mid		ΔP in H_{t+1}			
		Z1	**Z2**	**Z3**	**Z4**
ΔP in H_t	**Z1**	60 (-3)	38 (+4)	2 (-1)	<1
	Z2	4 (-1)	77 (+1)	19	<1
	Z3	<1	19	76 (+1)	5 (-1)
	Z4	<1	2	36 (+5)	62 (-5)
Residual Load - High		ΔP in H_{t+1}			
		Z1	**Z2**	**Z3**	**Z4**
ΔP in H_t	**Z1**	56 (-7)	41 (+7)	3	<1
	Z2	6 (+1)	77 (+1)	17 (-2)	<1
	Z3	<1	25 (+6)	68 (-7)	7 (+1)
	Z4	-	3 (+1)	27 (-4)	70 (+3)

Z1: ΔP < -10 €/MWh
Z2: -10 €/MWh <= ΔP < 0 €/MWh
Z3: 0 €/MWh < ΔP <= 10 €/MWh
Z4: ΔP > 10 €/MWh